Aerodynamic optimization of propellers for High Altitude Pseudo-Satellites

Adrián García, Jesús Gonzalo, Diego Domínguez, Deibi López, Alberto Escapa
Universidad de León, Aerospace Engineering Area, Campus de Vegazana S/n, León, 24071, Spain

Abstract

The propulsion system of High-Altitude Platform Stations or High-Altitude Pseudo-Satellites (HAPS) is commonly based on propellers. The properties of the atmosphere at those high altitudes and the characteristic speed of HAPS entail that the flight is performed at very low Reynolds numbers. Hence, the aerodynamic behavior of the propeller sections changes substantially from the hub to the tip of the blades. Under those circumstances, the ordinary methods to develop optimized propellers are not useful and must be modified. We present a method of propeller design adapted to HAPS features. It combines traditional solutions with modern numerical tools. Specifically, Theodorsen analytical theory is used to minimize induced drag. This process leaves one free parameter that it is fixed optimizing a cost function depending on the Reynolds number with a viscous-potential numerical code. It leads to an optimal determination of the geometrical characteristics of the propeller, i.e., chord and pitch distribution, increasing its total efficiency. The resulting algorithm has low computational requirements what makes it very appropriate for the preliminary design of HAPS missions, when it is necessary to simulate many different cases. That methodology has been applied to a relatively small HAPS airship with a wind speed of 10 m/s and required thrust of 100 N. The propeller is assumed to be made up of NACA4412 airfoils and the cost function to be minimized is given by the ratio of the 2D drag and lift coefficients. With those conditions we perform a parametric analysis where different combinations of diameters, thrust

Please cite this article in press as: García-Gutiérrez, A., Gonzalo, J., Domínguez, D., López, D., & Escapa, A. (2020). Aerodynamic optimization of propellers for High Altitude Pseudo-Satellites. Aerospace Science and Technology, 96, 105562, 10.1016/j.ast.2019.105562

coefficients, and propeller advance ratios are considered. Over a Reynolds number range from 10^3 to 10^6, the new method provides a gain about 5% in the propeller efficiency when compared with the ordinary design procedure that employs a constant Reynolds number. That gain is of utmost importance for HAPS operations, since, for example, it allows an increase in the payload of up to 25% for a 90 meters long airship.

Nomenclature

a	Sound speed
B	Number of blades
c	Blade chord
c_d	2D Drag coefficient
c_l	2D Lift coefficient
CDF	Cumulative distribution function
D	Propeller diameter
F	Cost function
G	Goldstein circulation function
HAPS	High-Altitude Pseudo-Satellites
K_P	Power coefficient, $\frac{P}{0.5\rho\pi R^2 V^3}$
K_Q	Torque coefficient, $\frac{Q}{0.5\rho\pi R^2 V^3}$
K_T	Thrust coefficient, $\frac{T}{0.5\rho\pi R^2 V^2}$
Ma	Mach number
n	Propeller revolutions per second
N_{crit}	Power
P	Power
PDF	Probability density function
Q	Torque
r	Geometry scale
R	Propeller radius
Re	Reynolds number

Please cite this article in press as: García-Gutiérrez, A., Gonzalo, J., Domínguez, D., López, D., & Escapa, A. (2020). Aerodynamic optimization of propellers for High Altitude Pseudo-Satellites. *Aerospace Science and Technology*, 96, 105562, 10.1016/j.ast.2019.105562

RMS	Root mean square
rpm	Revolutions per minute
SL	Sea level
T	Thrust
U	Resultant velocity at a blade element
V	Fluid velocity
α	Angle of attack
β	Blade angle from plane of rotation
Γ	Circulation, $\oint v \mathrm{d}\mathbf{x}$
η	Aerodynamic efficiency, $\frac{K_T}{K_P}$
λ	Advance ratio, $\frac{V}{\Omega R}$
μ	Kinematic viscosity
ρ	Air density
ν	Kinematic viscosity
σ_b	Blade solidity factor, $\frac{Bc}{2\pi R}$
Ω	Propeller Angular Velocity

Subscript

a	Aerodynamics loads
h	Value of the magnitude at the test altitude
i	Inertial loads
s	Value of the magnitude at 20 km of altitude

1. Introduction

With the recent evolution in efficiency and reliability of technologies such as solar panels, batteries, and brushless motors, stratospheric platforms —also called HAPS— might become fully operational in the next years. Projects like Airbus Zephyr$^{\mathrm{TM}}$ or Stratobus$^{\mathrm{TM}}$ are good examples on how the European industry is investing in these vehicles. Outside of Europe, other initiatives like the Odysseus [1] in USA, the Stratospheric Platform Airship of Japan [2],

Please cite this article in press as: García-Gutiérrez, A., Gonzalo, J., Domínguez, D., López, D., & Escapa, A. (2020). Aerodynamic optimization of propellers for High Altitude Pseudo-Satellites. *Aerospace Science and Technology*, 96, 105562, 10.1016/j.ast.2019.105562

Stratospheric Airship Program of South Korea [3], and Berkut HAA [4] in Russia confirm the tendency. All these projects benefit by the growing interest in electric airplanes [5]. The main advantages of HAPS platforms over traditional satellites are: (1) they have reduced costs, since their launch does not require expensive rockets, and they can be overhauled every 6/12 months; (2) they can offer better performance in some missions as, for example, those devoted to telecommunications and Earth observation [6].

The only feasible way to achieve such a high endurance is to use propellers for propulsion that are driven by electric motors. Some examples are the platforms Pathfinder [7], Centurion, Helios [8], Zephyr [9], and Stratobus [10], although the restricted character of those projects makes that the available data of the missions are very limited.

The electric motors are powered by the energy captured by solar panels placed on top of the airframe [11]. Once they reach the desired location for the provision of long-term services, they must stay there for periods of weeks, or months, in order to develop typical missions of communications or Earth observation. This condition of station-keeping, which can be achieved hovering or flying a prefixed circuit, is favored at high altitudes. There, the wind speed is minimum —mean wind speed [12] about 10-15 m/s— so less power is needed to keep the flight conditions.

There is not a general road-map for the development of HAPS propulsion system, in part, due to the several technologies that are involved: e.g., thermal control, electric systems, and aerodynamics. Traditionally [13], the first step is to determine the thrust required by the platform to perform its mission. Once this is done, it is choosen the optimal propeller to generate that thrust [14]. This propeller is designed with some specific dimensions over a given range of rpm and torque. Then, a motor with optimal performance at that range of rpm/torque could be selected. Finally, the thermal and mechanical behavior of the coupled system is determined. In this research we will follow that approach, focusing on the part related to an optimal propeller design for HAPS.

Propellers have been extensively used for aircraft propulsion during the XX

Please cite this article in press as: García-Gutiérrez, A., Gonzalo, J., Domínguez, D., López, D., & Escapa, A. (2020). Aerodynamic optimization of propellers for High Altitude Pseudo-Satellites. *Aerospace Science and Technology*, 96, 105562, 10.1016/j.ast.2019.105562

century and remain as one of the most efficient methods [4] of propulsion for subsonic flight. Propellers for conventional aircrafts operate at large Reynolds numbers; then, each propeller section can be characterized by the same airfoil curves [15] $\alpha - c_l$ and $c_l - c_d$, obtained for an averaged constant Reynolds number. In contrast, the flight of the HAPS is performed at very low Reynolds [16] numbers —in the range from 10^4 to 10^5. This is the result of a combination of the low atmospheric density in the stratosphere with a low flying speed. Under these circumstances, the operating Reynolds number falls in the range where laminar to turbulent transition occurs and viscous forces play a key role in the flow characterization. Some of its most relevant effects are [17, 18]:

1. Rapid descent of maximum lift-to-drag ratio due to thick boundary layers.
2. Symmetrical airfoils experience non-linear phenomena at small attack angles.
3. Flow separation occurs with long laminar separation regions.
4. Sensibility of the flow to free-stream turbulence is increased.

Hence, in this low regime, the change in the value of the Reynolds number of the propeller sections is very relevant. That change is a consequence of the increase of linear velocity when running from the hub to the tip of the blades.

This variation of the Reynolds number along the blade is not significant in the high regime, hence it is not taken into account in the design of conventional propellers. So, the use of those conventional design methods for HAPS will not provide the best possible aerodynamic performance. A non-optimized design will unnecessarily increase drag, penalizing the power system requirements, and compromising the whole mission feasibility. For this reason, an alternative design approach is required.

The aim of this paper is to construct such an alternative for the optimized design of HAPS propellers. Specifically, the design methodology must have the following characteristics:

1. It should be able to tackle the low Reynolds phenomena and changes in Reynolds number along the propeller blade airfoil sections.

Please cite this article in press as: García-Gutiérrez, A., Gonzalo, J., Domínguez, D., López, D., & Escapa, A. (2020). Aerodynamic optimization of propellers for High Altitude Pseudo-Satellites. *Aerospace Science and Technology*, 96, 105562, 10.1016/j.ast.2019.105562

2. It should be easily modified with different optimization criteria.
3. It should use few computational resources.

The structure of the paper is as follows. In Section 2, the different approaches currently used for the design of stratospheric propellers are summarized and the proposed design algorithm is also presented. Different issues with major effect on the propeller design process are studied in Section 3: wind velocity plays a key role and will be carefully analyzed, as well as the effect of low Reynolds aerodynamics on airfoils performance. In Section 4 the algorithm is applied to a case of study where we consider the optimized propeller with a NACA4412 airfoil for a small HAPS airship. An analysis of the relevance of the results and their impact on the platform performance can be found in Section 5. Finally, the conclusions are summarized in Section 6.

2. Design methodology of HAPS propellers

2.1. Current approaches

Different approaches have been proposed in order to design a propeller [19]. Most of them are based on the inverse design method which defines the required blade geometry for a predefined operational point, trying to optimize the total efficiency of the propeller η.

It can be described as the product of two terms, each one related to the viscous η_v and induced losses η_i. Usually, the condition imposed during the design process is to minimize the induced drag —maximizing η_i— and this can be done as described by Theodorsen [20]. Based on this method, a comprehensive analytical study about the design of propellers can be found in Wald [21]. In that research it is described how the optimal propeller should create helical vortex sheets with a certain shape and explained the method to solve the inverse design problem. Some considerations about the performance are done without taking into account Reynolds number variations along the propeller sections.

Some recent studies have aimed at adapting those methods to low Reynold number regime. As example of this, Morgado [22] introduced a three-dimensional

Please cite this article in press as: García-Gutiérrez, A., Gonzalo, J., Domínguez, D., López, D., & Escapa, A. (2020). Aerodynamic optimization of propellers for High Altitude Pseudo-Satellites. *Aerospace Science and Technology*, 96, 105562, 10.1016/j.ast.2019.105562

flow equilibrium model, and Mac Neill [23] introduced the Viterna and Corrigan flat plate theory [24], the Snelt *et al* model [25], and other corrections due to rotational effects. However, there is no general agreement about how to tackle the viscous losses η_v. A common procedure is to try different designs [26, 23], choosing the one with the best performance. Other authors —e.g., Park [27] and Jiao [28]— use genetic/statistical algorithms at the cost of computational time. Again, no direct treatment of the low Reynolds phenomena or change in aerodynamic performance along blade sections is considered during the optimization phase.

Starting from these approaches, we extend the method by Wald[21] together with the corrections used in Mac Neill [23], and a specific analysis of a cost function depending on the viscous losses. It will allow optimizing the propeller efficiency in the low Reynolds regime, as we show in the next section.

2.2. Proposed optimization method

The optimization algorithm is based on the well-known Theodorsen's theory [15, 21]. The optimal radial distributions of blade's chord and lift coefficient are calculated by means of the Goldstein [29] distribution G for a given thrust coefficient K_T, advance ratio λ, and number of blades B. In Figure 1 we have displayed some examples of this distribution for different values of λ and B. The former mentioned distribution is optimal in the sense that induced drag [30] is minimized.

Its only requirement is to provide a given value of the product $c_l \cdot \sigma_b$, where σ_b represents the blade solidity. There are two variables for only one constraint, so there is a degree of freedom —c_l or σ_b— that fixes the value of the other variable, and it can be chosen in such a way that the optimum efficiency c_l/c_d is achieved. When the propeller is expected to operate at high Reynolds regime, the approach usually taken is to suppose that the aerodynamic coefficients are independent of the Reynolds number. In that case, the c_l of maximum efficiency is easily calculated using the airfoil's polar, common for all the sections of the propeller. However, as it was mentioned in Section 1, this approach is not

Please cite this article in press as: García-Gutiérrez, A., Gonzalo, J., Domínguez, D., López, D., & Escapa, A. (2020). Aerodynamic optimization of propellers for High Altitude Pseudo-Satellites. *Aerospace Science and Technology*, 96, 105562, 10.1016/j.ast.2019.105562

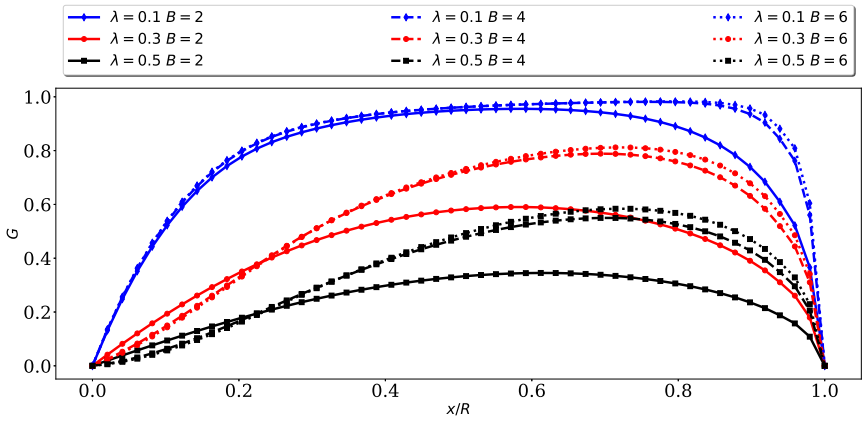

Figure 1: Goldstein [29] circulation function, calculated as per Ribner and Foster [30], provides the optimal circulation along the blade to produce minimum induced losses. It is shown for different combinations of number of blades B and advance ratios λ.

suitable for the low Reynolds regime [17] in which the propellers operate in the stratosphere. In that case, the aerodynamic performance is highly dependent from the Reynolds number —as it will be shown later in Section 4, Figure 11.

To tackle this difficulty, and to have a design method for HAPS propellers, the first step is to select the airfoils that make up each propeller section. Once the airfoil set is selected, the $\alpha - c_l$ and $\alpha - c_d$ curves are calculated for a wide ranges of Reynolds and Mach numbers. More information about how to obtain those input data is given in Subsection 3.1 but typically, potential numerical codes are used, although they can also be provided by experimental tests. The exact Reynolds range which will be needed is not known until the final design is reached, but, due to the low time required by the potential flow solvers, a large enough range can be calculated —usually, $\mathrm{Re} \in [10^4 - 10^6]$. On the other hand, the propeller's tip Mach limit is fixed to be 0.7, so $\mathrm{Ma} \in [0, 0.7]$. These results will be used to interpolate the values of c_l and c_d for each combination of α, Re, and Ma that could be needed during the design process. It is also possible, e.g., [31], to calculate the aerodynamic coefficients on demand —without interpolation— and for the exact Reynolds number. That

Please cite this article in press as: García-Gutiérrez, A., Gonzalo, J., Domínguez, D., López, D., & Escapa, A. (2020). Aerodynamic optimization of propellers for High Altitude Pseudo-Satellites. *Aerospace Science and Technology*, 96, 105562, 10.1016/j.ast.2019.105562

approach can be used to increase the accuracy of the final design. However, the potential flow code has to be executed every time the aerodynamic coefficients are needed [32], so there is a significant increase in the computational time. Usually [33, 22, 34], only one kind of airfoil is used along the propeller aiming at simplicity of its design and manufacture, although the proposed method can be extended to the general case without difficulties.

Then, it is time to calculate the pitch angle and chord length along the blade. This, together with some other input design parameters —e.g. number of blades, rpm, or wind speed— determines the performance of the propeller: thrust, torque and efficiency. The role played by wind speed is of paramount importance. Its intensity not only modifies the thrust required by the platform to perform station keeping, but also the Reynolds that each blade section experiences and the advance velocity of the propeller —the relative velocity between the propeller and surrounding air. For these reasons, it is required to analyze the characteristics of the wind at the region in which the mission will be done. A preliminary study of the wind properties in the stratosphere is presented in Section 3.2.

Theodorsen theory [15, 20, 21] receives as input the ideal thrust coefficient $K_{T\,i}$ that is desired —i.e., the ideal thrust T_i that the propeller would generate if there were no aerodynamic drag— together with the advance ratio, and number of blades. In order to generate this thrust, the mentioned $\sigma_b \cdot c_l$ distribution is required. Thus, the problem is a two-dimensional optimization in which the constraint is to achieve a determined $c_l \cdot c$ value while some cost function $F(\mathrm{Re})$ is maximized:

$$\begin{aligned} \max_{c_l, c} \quad & F(c_l, c_d) = F(\mathrm{Re}), \\ \text{s.t.} \quad & c_l(\mathrm{Re}) \cdot \sigma_b = G(K_T,\, \lambda), \\ & \mathrm{Re} = \frac{\rho v c}{\mu} = \frac{2\pi\sigma_b}{B}\frac{\rho v R}{\mu}. \end{aligned} \tag{1}$$

In the present study, we use the cost function $F(\mathrm{Re}) = c_l/c_d$ to maximize the efficiency η_ν. Other cost functions can be employed with no problem. For example, taking $F(\mathrm{Re}) = c_l^{3/2}/c_d$ can reduce the propeller dimensions[35].

Please cite this article in press as: García-Gutiérrez, A., Gonzalo, J., Domínguez, D., López, D., & Escapa, A. (2020). Aerodynamic optimization of propellers for High Altitude Pseudo-Satellites. *Aerospace Science and Technology*, 96, 105562, 10.1016/j.ast.2019.105562

This problem can be attacked directly by discretizing the possible chord values. Specifically, for each cord value the Reynold number is computed. It allows calculating c_l and c_d, by interpolation of the airfoil data with the corrections given in MacNeill [23]. Then it is obtained $F(\mathrm{Re})$. Each section generates a certain amount of drag that modifies the real thrust of the propeller. As a consequence, it is needed to iterate the desired value of T_i until the required final thrust is reached.

In Figure 2, the flow diagram of the optimization algorithm is shown with all its relevant parts.

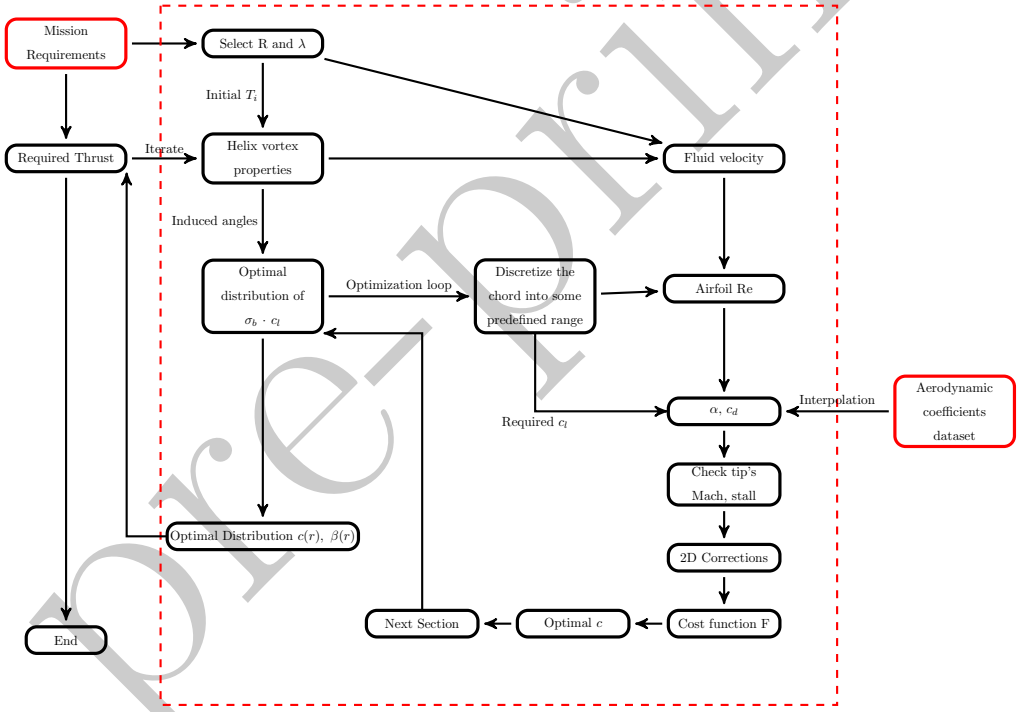

Figure 2: Flow diagram of the proposed optimization algorithm.

The optimization for a given R, K_T and λ, once the airfoil maps have been calculated, relies on analytic equations and no additional simulations are needed. As a consequence, the time required is low and the algorithm can be used to do a parametric sweep as it is exemplified in Section 4. With this analysis a

Please cite this article in press as: García-Gutiérrez, A., Gonzalo, J., Domínguez, D., López, D., & Escapa, A. (2020). Aerodynamic optimization of propellers for High Altitude Pseudo-Satellites. *Aerospace Science and Technology*, 96, 105562, 10.1016/j.ast.2019.105562

careful selection of the diameter, advance parameter, and number of blades can be done, taking into account the effect of propeller's rpm in the brushless motor performance.

It is worth mentioning that the optimization is performed for a given thrust, not a specific K_T. Although all the inviscid optimization can be done with dimensionless parameters, the length scale influences the airfoil's aerodynamic coefficients and, thus, the optimization result depends on the radius of the propeller and cannot scale with the length.

3. Setup of the optimization method for HAPS propellers

The setup of the proposed algorithm needs two basic external inputs: one is the mission requirements, particularly through the necessary thrust; the second one is the $\alpha - c_l$ and $\alpha - c_d$ curves of the airfoils composing the propeller for the different operating Reynolds numbers (Figure 2, red boxes).

Those inputs are determined by the nature of the airframe under consideration, since the new propeller design algorithm can be employed for any kind of platform. In particular, when applied to HAPS it is necessary to pay attention to the wind distribution, which is a key factor in the mission definition, and to the determination of the aerodynamic properties of the airfoils at low Reynolds numbers. The models to account for them are complex and face with the difficulty of a lack of experimental data.

In this scenery, we have considered two simple ways to model the stratospheric wind and the airfoil behavior at low Reynolds numbers. It is enough to show the general advantages of the new method of HAPS propeller design over the conventional one, independently that the proposed algorithm can be applied to more refined input models as they are available with HAPS flights increasing.

3.1. Airfoils aerodynamic performance at Low Reynolds

As it has been mentioned, the algorithm requires the aerodynamic coefficients of the airfoil for a given range of Re, Ma, and angles of attack. Generally

Please cite this article in press as: García-Gutiérrez, A., Gonzalo, J., Domínguez, D., López, D., & Escapa, A. (2020). Aerodynamic optimization of propellers for High Altitude Pseudo-Satellites. *Aerospace Science and Technology*, 96, 105562, 10.1016/j.ast.2019.105562

speaking, viscous potential codes —e.g., XFOIL [36], Javafoil [37], or Eppler's code [38]— can be used at preliminary design stages and their validity [27, 39, 40] has been proven for different airfoils. Their main advantages are the low time of computation, their simple use, and the multiple cases that can be analyzed.

Alternatively, there are other options to obtain those data. For example, one could employ:

1. CFD simulations, most of them using RANS turbulence models [19, 26, 41].
2. Experimental tests using wind tunnels [42, 43].

However, usually the use of these methods is inviable for the broad range of Reynolds and Mach numbers that should be considered during the design process for each airfoil [44]. The main reason is its high cost both in time and resources, particularly in the case of experimental tests. Nevertheless, they can be used as a complementary data source and as a validation tool [33] for the results obtained by the potential codes.

In fact, although the particular details provided by any of those methods are different, they give the same global picture. We made some test in that direction by using the NACA4412 airfoil (see next section) in the new low Reynolds wind tunnel built at the University of León —See Figure 3. ULE's tunnel is designed to operate with low wind speeds —lower than 5 m/s— and low turbulence intensity —lower than 0.5%, so Reynolds values between 4×10^4 and 1.1×10^5 can be obtained. The cross-sectional area is $0.54\,\mathrm{m}^2$ —60×90 cm width and height respectively. With this section, the range of velocities that can be achieved in the test chamber is between 3 to 7 m/s, setting the wing surface to 60×25 cm of span and chord respectively. The airfoil had been manufactured with expanded polystyrene. An additional treatment has been added to create a smooth surface, consisting of a sealant that can be polished.

The results of the test at three different Reynolds 4×10^4 (Figure 4), 7.5×10^4 (Figure 5), and 10^5 (Figure 6) are displayed together with the values obtained from a potential solver and other experimental data available in the literature.

Figure 3: Wind tunnel in which the airfoils were tested. Reynolds values between $4\,10^4$ and $1.1\,10^5$ can be obtained

The figures show how the low Reynolds increase the results variability [45]: each of the experimental datasets has different values, what indicates the dependence [45, 46] between aerodynamic coefficients and the flow conditions [16] created by the wind tunnel. This variability could be explained based on a large number of reasons, the most relevant are the appearance of laminar separation bubbles [46] and the high sensibility of the location of the laminar to turbulent transition point to the wind tunnel test conditions.

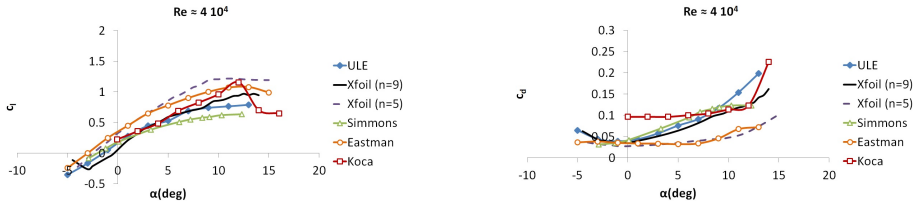

Figure 4: c_l and c_d values of the NACA4412 estimated for $\mathrm{Re} = 4 \times 10^4$ using XFOIL ('$\mathrm{N_{crit}}$' = 5 and 9) and test results. Additional datasets from Simmons [47], Eastman [48], and Koca [49] have been added.

Please cite this article in press as: García-Gutiérrez, A., Gonzalo, J., Domínguez, D., López, D., & Escapa, A. (2020). Aerodynamic optimization of propellers for High Altitude Pseudo-Satellites. *Aerospace Science and Technology*, 96, 105562, 10.1016/j.ast.2019.105562

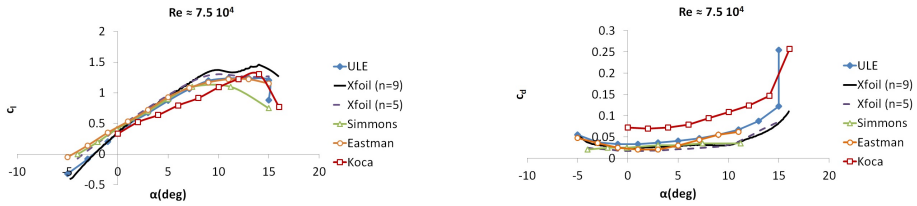

Figure 5: c_l and c_d values estimated for Re $= 7.5 \times 10^4$ using XFOIL ('N_{crit}' = 5 and 9) and test results. Additional datasets from Simmons [47], Eastman [48], and Koca [49] have been added.

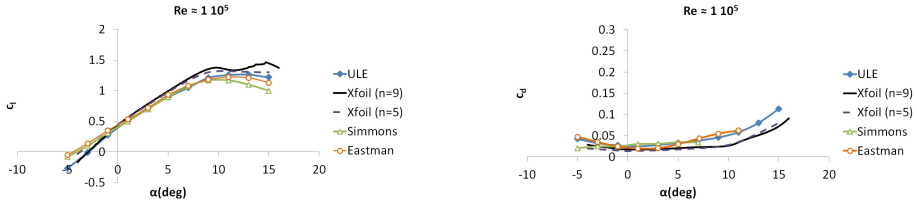

Figure 6: c_l and c_d values estimated for Re $= 10^5$ using XFOIL ('N_{crit}' = 5 and 9) and test results. Additional datasets from Simmons [47], Eastman [48], and Koca [49] have been added.

As it can be seen, the results obtained using the potential solver lay between the different test results, what, besides the advantages pointed out formerly, justifies its use within the scope of this research.

3.2. Mission requirements: stratospheric winds

Wind speed plays a key role in the determination of not only the required thrust but also the Reynolds number and the propeller advance parameter. It is well-known that stratospheric winds are weaker than those ones in the troposphere, and that they exhibit important differences depending on the exact geographical location. However, it is difficult to find in the literature quantitative studies about the global wind intensity at the height of 20 km in the stratosphere. The main reason is probably that only in recent times the interest to flight at this altitude has been renewed.

Please cite this article in press as: García-Gutiérrez, A., Gonzalo, J., Domínguez, D., López, D., & Escapa, A. (2020). Aerodynamic optimization of propellers for High Altitude Pseudo-Satellites. *Aerospace Science and Technology*, 96, 105562, 10.1016/j.ast.2019.105562

Wind distribution in the stratosphere can be obtained through the statistical analysis of the available meteorological data from the NCEP/NCAR reanalysis project [50]. They are available from 1948/01/01 up to the present day, 4 times per day, and its spatial resolution is 2.5° in latitude and longitude. The available pressure levels are in the range between 10^3 and 10 mbar, so the operational level —around 20 km or 55 mb— falls within the range.

The most relevant results from the statistical analysis can be found in figures 7 and 8. In Figure 7, it can be seen how the wind intensity is not symmetric with respect to the equator. While at latitudes lower than 5°, 99% of the time wind speed is less than 20 m/s, at latitudes around −5°, the 15% of the time, wind speeds are higher than 20 m/s. This anti-symmetry requires to define the local domain of the mission in order to maximize the flight efficiency.

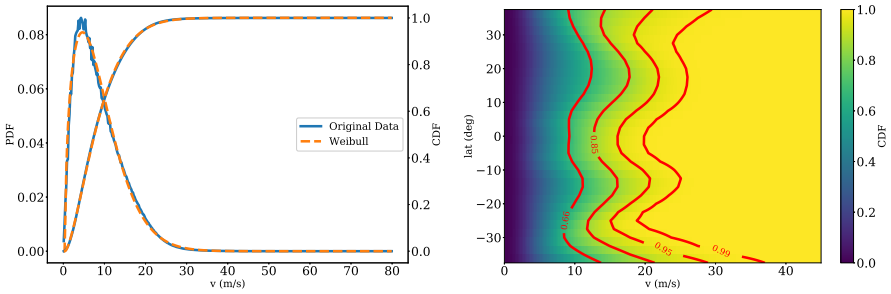

Figure 7: Left panel: calculated probabilistic density function PDF and cumulative distribution function CDF of the wind speed for all the latitudes between ± 40° for a pressure level of 50 mbar. It also shows the fitted Weibull [51] distribution. Right panel: bi-dimensional CDF of the speed intensity in function of the latitude.

In most of the design algorithms —as in the present study— the ideal propeller is designed for a particular wind speed. This makes sense as, for example, a common mission requirement for an stratospheric airship is to perform station keeping in the presence of a stationary wind field of constant intensity. Thus, the whole mission performance relies on a good selection of the speed at which the propeller is supposed to operate most of the time.

In the case of airships, the wind mean speed for that altitude, or its root mean

Please cite this article in press as: García-Gutiérrez, A., Gonzalo, J., Domínguez, D., López, D., & Escapa, A. (2020). Aerodynamic optimization of propellers for High Altitude Pseudo-Satellites. *Aerospace Science and Technology*, 96, 105562, 10.1016/j.ast.2019.105562

square RMS value, provides significant order of magnitude. As it is shown in Figure 8 for different combinations of latitude and longitude the RMS oscillates between 7 m/s and 18m/s while the mean velocity values yields between 6 m/s and 15 m/s.

Once the wind statistical study is performed for the places where the mission will be developed, the former approach could be enhanced to consider the probabilistic wind distribution. This distribution can be discretized, and, instead of looking for the optimal λ at a given wind speed, a weighted sum —given by the probability of each wind value— would be maximized. The real velocity at which the propeller will work depends on different factors that are impossible to fully estimate at the preliminary design phase e.g., station-keeping trajectory strategy, vehicles shape configuration.

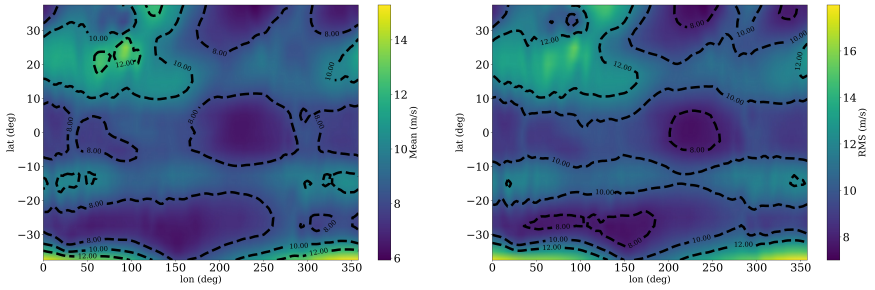

Figure 8: Characteristic velocities obtained after the statistical analysis of NCEP/NCAR [50] weather data from 1948 to 2019 for a pressure level of 50 mbar —about 20 km. Left panel: Wind mean velocity. Right panel: RMS.

4. Optimized propeller design for a small HAPS airship with a NACA4412 airfoil

Next, we exemplify the application of the optimized algorithm for propeller design to a small HAPS airship. Accordingly to the last section we need as main inputs the wind speed and the aerodynamic characteristic of the airfoils forming the propeller.

With respect to the wind, we select a value of 10 m/s, entailing a flight

Please cite this article in press as: García-Gutiérrez, A., Gonzalo, J., Domínguez, D., López, D., & Escapa, A. (2020). Aerodynamic optimization of propellers for High Altitude Pseudo-Satellites. *Aerospace Science and Technology*, 96, 105562, 10.1016/j.ast.2019.105562

speed of the opposite sign. It leads to a stationary station-keeping condition with respect to the ground. A speed of 10 m/s is approximately the mean value for the regions located at latitudes about 20° and longitudes between 0° and 150°E. With a 400 kg payload, a total length of 90 m and using two propellers, the required thrust by each of them is approximately 100 N.

As regards the airfoil, we will consider that the propeller sections are given by the NACA4412 airfoil. This airfoil has been extensively used for low Reynolds propellers [23, 49, 52, 53]. Following the nomenclature of the NACA four-series airfoils, its maximum camber is 4% of the chord, and it is located at $0.4c$ with a maximum thickness of $0.12c$.

The *a priori* Reynold numbers of operation run from 10^3 to 10^6, and the selected cost function to account for the viscous losses is $F(\mathrm{Re}) = c_l/c_d$. In this range we have computed the aerodynamics characteristics of the NACA4412 airfoil with the help of XFOIL. As we have remarked previously, at this low Reynolds number regime the effect of a Re variation on the cost function $F(\mathrm{Re})$ is very significant.

This fact can be corroborated in Figure 9, where it is contrasted the behavior of $F(\mathrm{Re})$ for high Reynolds numbers. As it can be seen, at those values, $F(\mathrm{Re})$ is an almost constant function with respect to Re.

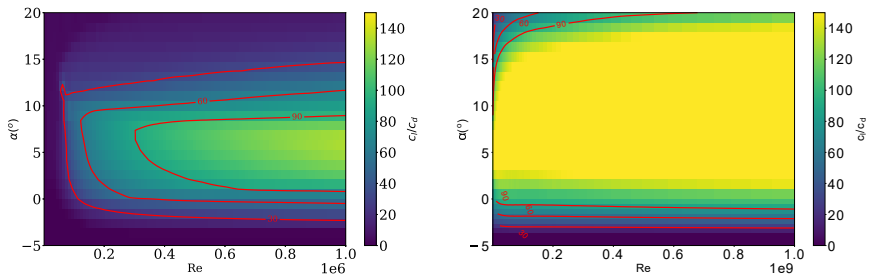

Figure 9: c_l/c_d values predicted by XFOIL for the NACA4412 at Mach = 0.2 as a function of the Reynolds number and attack angle. In each of the figures, isocontours with values of 90, 60 and 30 are plotted.

It is not the case when the Reynolds number is low, where the coefficients

Please cite this article in press as: García-Gutiérrez, A., Gonzalo, J., Domínguez, D., López, D., & Escapa, A. (2020). Aerodynamic optimization of propellers for High Altitude Pseudo-Satellites. *Aerospace Science and Technology*, 96, 105562, 10.1016/j.ast.2019.105562

changes are notorious. In that range, more simulations should be done when compared to high Reynolds. So, instead of calculate the coefficients for equispaced Reynolds number values, it is recommended to increase the resolution at low Reynolds numbers.

For the present case, the Mach values are linearly equispaced with steps of 0.1 between 0 and 0.7 while the Reynolds values are logarithmically spaced in 200 bins between 10^3 and 10^6. Once these datasets are calculated, a linear interpolation is used to calculate the coefficients for the Ma and Re numbers that the algorithm requires. The chord is also discretized, so it only takes values up to 1.5 m in steps of 5 mm. These resolutions have proven to be enough for preliminary design. As it has been mentioned, instead of interpolating, a potential code can be called every time an aerodynamic coefficient is required, what entails about 10^6 calls for our algorithm. That number justifies the use of linear interpolation in order to reduce the computational load, although some accuracy is lost. However, the accuracy of the interpolation can be enhanced by increasing the number of control points. To assess the accuracy of our interpolatory scheme some of the propellers designs have been recomputed halving the original Reynolds discretization. We have verified that the geometry is not altered significantly and the variations in the aerodynamic efficiency are negligible.

A parametric sweep has been done in order to determine how the propeller performance is affected by changes in the radius —from 3.5 m up to 8 m in steps of 0.5 m—, advance parameter —from 0.1 up to 0.6 in steps of 0.05– and number of blades —between 2 and 6. Thus, for the different parameter combinations, the optimal design is obtained and compared with the others to determine which one is the true optimal. In Figure 10 we displayed the results: the effect of the number of blades is notable, being the propellers with 2 blades those who offers the best performance. Other cases in which the Reynolds is higher —as consequence of higher wind speed and required thrust— show that the effect of the number of blades on the maximum performance that can be achieved is negligible, just modifying the rpm at which that maximum is reached.

Please cite this article in press as: García-Gutiérrez, A., Gonzalo, J., Domínguez, D., López, D., & Escapa, A. (2020). Aerodynamic optimization of propellers for High Altitude Pseudo-Satellites. *Aerospace Science and Technology*, 96, 105562, 10.1016/j.ast.2019.105562

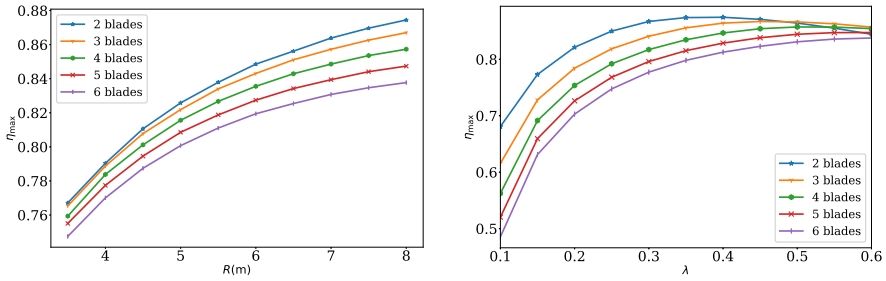

Figure 10: Variation of the maximum efficiency for different number of blades. Left panel: in function of the propeller radius. Right panel: in function of the advance ratio.

An important question, which is the corner stone of the present study, is what happens if the propeller is designed without taking into account the low Reynolds effects. In Figure 11, it is shown how the Reynolds number varies along the propeller blade for different radius. It can be seen in the same figure how the aerodynamic efficiency notably changes in the considered Reynolds range.

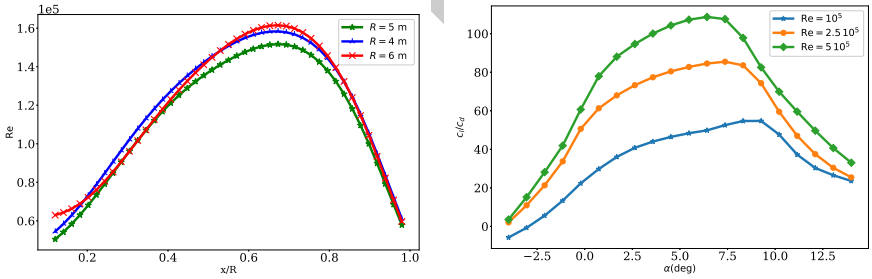

Figure 11: Left panel: the Reynolds distributions along the propeller blade are shown for the optimal design with different blade radius and $N = 4$. Right panel: aerodynamic efficiency of the NACA4412 for three different Reynolds number.

The effect of considering during the design process a constant Reynolds number for all the blade sections can also be analyzed. The algorithm must be modified: in this case there is only one curve $\alpha - c_l/c_d$ for all the blade sections, so the angle of maximum efficiency is easily found. Thus, the algorithm coincides with the conventional methodology —described in detail by Wald [21]— when the hypothesis of a constant Reynolds along the blade is assumed. For

Please cite this article in press as: García-Gutiérrez, A., Gonzalo, J., Domínguez, D., López, D., & Escapa, A. (2020). Aerodynamic optimization of propellers for High Altitude Pseudo-Satellites. *Aerospace Science and Technology*, 96, 105562, 10.1016/j.ast.2019.105562

traditional propellers, the high Reynolds at which they usually operate justifies the use of that hypothesis. However, in the stratospheric case, it will affect the aerodynamic performance, since the Reynolds number varies appreciably along each blade section. In Figure 12, the results are compared when using the traditional method instead of the proposed optimization algorithm. The decrease in aerodynamic efficiency is larger than 5 percent in a broad range of radius and rpm.

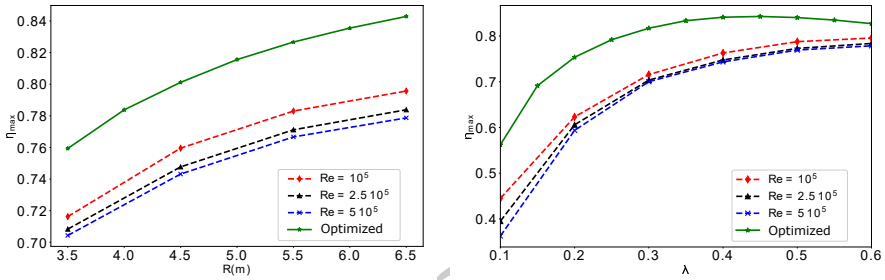

Figure 12: Optimal design created using the proposed optimization algorithm —solid line— is compared with the performance of designs at constant Reynolds —dashed lines— for $N = 4$. Variation of the maximum propeller efficiency. Right panel: in function of the blade radius. Left panel: in function of λ.

The procedure described above allows obtaining a particular optimum design. For example, in Figure 13 we have represented a propeller with $R = 4\,\mathrm{m}$, $\lambda = 0.3$, and $B = 4$ taking into account the chord and pitch angle distributions derived from the algorithm.

Although it is out of the scope of this investigation entering into the constructive aspects and real performance of the designed propeller, we have performed two simple preliminary analysis. First, a structural study has been done using the beam theory as first approximation. Each section suffers from aerodynamic and inertial loads that originates stress. This can be estimated using the methodology proposed by Ketcham [54]. Due to the low rotational speed, the stress values found in each of the optimal designs are very low when compared with typical critical failure values [55].

Please cite this article in press as: García-Gutiérrez, A., Gonzalo, J., Domínguez, D., López, D., & Escapa, A. (2020). Aerodynamic optimization of propellers for High Altitude Pseudo-Satellites. *Aerospace Science and Technology*, 96, 105562, 10.1016/j.ast.2019.105562

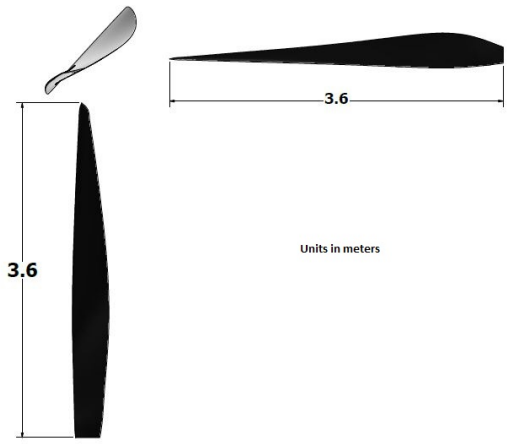

Figure 13: Drawing of one of the optimal propellers. The scale of the front view is 2.5 times bigger than the other two.

Second, to test the designed propellers at sea level conditions it is required to achieve the dynamic similarity between the test and operational conditions. The relevant physical parameters are shown in Table 1. With that 8 parameters, 5 dimensionless groups can be defined as in Table 2.

Symbol	Parameter	Dimensions
D	Propeller Diameter	l
n	Revolutions per unit time	t^{-1}
V	Fluid velocity	lt^{-1}
ρ	Density	ml^{-3}
ν	Kinematic viscosity	$l^2\ t^{-1}$
a	Sound speed	lt^{-1}
T	Thrust	mlt^{-2}
Q	Torque	$ml^2\ t^{-2}$

Table 1: Parameters that characterized the propeller design.

Symbol	Group	Definition
Re	Reynolds	$\frac{\rho V D}{\nu}$
Ma	Mach	$\frac{V+\pi D n}{a}$
λ	Advance parameter	$\frac{V}{2\pi n D}$
K_T	Thrust coefficient	$\frac{2T}{\rho\pi(D/2)^2V^2}$
K_Q	Torque coefficient	$\frac{2Q}{\rho\pi(D/2)^3V^2}$

Table 2: Dimensionless groups defined using the parameters from Table 1.

Due to the π-Buckingham theorem [56], we have the functional dependencies $K_T = f_1(\mathrm{Re}, \mathrm{Ma}, \lambda)$ and $K_Q = f_2(\mathrm{Re}, \mathrm{Ma}, \lambda)$. In order to achieve the required dynamic similarity, these three parameters (Re, Ma, λ) should be similar in

Please cite this article in press as: García-Gutiérrez, A., Gonzalo, J., Domínguez, D., López, D., & Escapa, A. (2020). Aerodynamic optimization of propellers for High Altitude Pseudo-Satellites. *Aerospace Science and Technology*, 96, 105562, 10.1016/j.ast.2019.105562

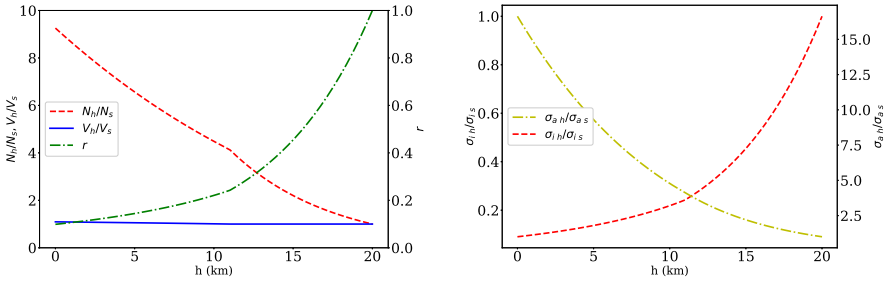

Figure 14: Dependence of the scaled propeller functions with the test altitude h. Left panel: wind speed, geometry scale r, and rotational speed. Right panel: aerodynamic σ_a and inertial σ_i stresses.

both situations. Denoting with the suffix "s" the variables at the operational altitude and with the suffix "h" the variables at the test altitude, it is obtained:

$$\mathrm{Re}_s = \mathrm{Re}_h \implies \frac{V_s}{V_h} \approx \frac{\mu_s}{\mu_h}\frac{1}{r} \tag{2}$$

$$\mathrm{Ma}_s = \mathrm{Ma}_h \implies \frac{V_s + \pi D_s n_s}{a_s} \approx \frac{V_h + \pi D_h n_h}{a_h} \implies \frac{V_s}{V_h} \approx \frac{(a_s/a_h)^2 + \lambda_h}{\frac{a_s}{a_h}(\lambda_h + 1)} \tag{3}$$

$$\lambda_s = \lambda_h \implies \frac{n_s}{n_h} \approx \frac{\mu_s}{\mu_h}\frac{1}{r^2} \tag{4}$$

in which $r = \frac{D_h}{D_s}$ is the geometry scale.

In Figure 14 it is shown how these three variables should vary depending on the test altitude to reproduce the conditions of an operational altitude of 20 km. When the test is performed at SL conditions, the model length should be around 0.1 times the original size and it should rotate 9.2 times faster. It is important to note that the Mach similarity equation depends on the propeller advance parameter during the operation.

5. Discussion

It is worth to analyze the results obtained in the last section from the perspective of the mission performance. Our new optimization method for HAPS

Please cite this article in press as: García-Gutiérrez, A., Gonzalo, J., Domínguez, D., López, D., & Escapa, A. (2020). Aerodynamic optimization of propellers for High Altitude Pseudo-Satellites. *Aerospace Science and Technology*, 96, 105562, 10.1016/j.ast.2019.105562

propellers has shown that it is possible to improve the propeller efficiency about a 5%, when compared with the conventional design method, by a proper selection of the propeller features. That increase translates into an enhancement of the mission capabilities in at least two essential aspects.

On the one hand, there is a direct increment in the range and endurance of the mission. Indeed, similar arguments as those employed in Traub [57] show that for electric propulsion these two functions are proportional to the efficiency raised to the power of the battery discharge parameter. Its particular value depends on the kind of battery and the temperature, but a common value of 1.3 can be assumed for typical lithium–polymer batteries [57]. It entails that an increase about 5% in the efficiency stems an increment of about 6.5% in the range and endurance.

On the other hand, the payload of the mission can be also increased in a significant way. Although a complete study would require to take into account all the particular details of the mission (e.g., airframe dimensions, daylight hours, solar panels surface, etc.), we can obtain an estimation on the basis that the thrust required for the mission remains constant. Under that proviso, an increment in the efficiency reduces the power consumption of the propeller. Thus, increasing the propeller efficiency is equivalent to improving the battery energy density. The dependency of vehicle size, payload mass, and specific capacity of the batteries were studied by Gonzalo *et al* [6].

In Figure 15 we translate that study in terms of the propeller efficiency and show that an improvement in efficiency notably increases the maximum payload for a given characteristic length. It is calculated using a conservative assumption that 80% of the platform's power consumption is due to the propulsion system. It can be seen in the figure that an improvement of the propeller efficiency of a 5% can increase by a 25% the payload mass. It would be the case for the smaller airship considered in the last section (design point in Figure 15).

Although our previous discussions are mainly based on the particular results derived for a small HAPS airship with a NACA4412 airfoil, their features seem to show a general trend. For example, we have analyzed the changes in the results

Please cite this article in press as: García-Gutiérrez, A., Gonzalo, J., Domínguez, D., López, D., & Escapa, A. (2020). Aerodynamic optimization of propellers for High Altitude Pseudo-Satellites. *Aerospace Science and Technology*, 96, 105562, 10.1016/j.ast.2019.105562

of the new algorithm when choosing a different airfoil (E66) and a different cost function —$F(\mathrm{Re}) = c_l^{3/2}/c_d$. We have obtained no substantial variation, less than 1%, for the propeller efficiency.

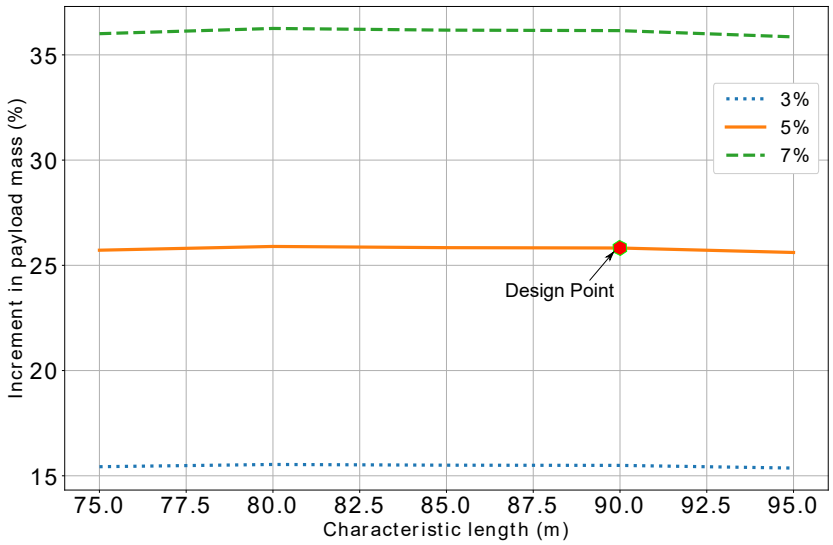

Figure 15: Increment in the payload mass that can be achieved when increasing the propeller efficiency of a stratospheric airship by a 3%, 5% or 7%. Similar results were found in the case of an airplane.

From the operations point of view, it is also important to discuss how the obtained propeller design is adapted to the mission ascending and descending phases. The change in the altitude stems a variation in the vehicle's drag that is proportional to the atmospheric density. Hence, the required thrust in these phases shows a similar variation. It can be controlled by adjusting the revolutions of the electric motor. In addition, the Reynolds number also varies as a consequence of the change in the atmospheric properties.

Both parameters affect the propeller efficiency that will not be working in its design point. However, the variations of η and n with the altitude have been calculated and they are not relevant for a standard stratospheric vehicle (less than 1%).

Please cite this article in press as: García-Gutiérrez, A., Gonzalo, J., Domínguez, D., López, D., & Escapa, A. (2020). Aerodynamic optimization of propellers for High Altitude Pseudo-Satellites. *Aerospace Science and Technology*, 96, 105562, 10.1016/j.ast.2019.105562

It entails that our optimized design works properly for low altitudes. In contrast, as it was shown in Section 4, the conventional methods —valid at SL conditions— would degrade the propeller efficiency accordingly the Reynolds number decreases, because at those regions Re variations in the propeller sections are relevant.

This analysis can be sharpened considering the wind variability in the ascending and descending phases. However, the main conclusion is kept: There is no significant penalization in those phases by using a propeller optimized for stratospheric conditions.

6. Conclusions

This study has identified how traditional methods used for propeller design are penalized because they do not consider the low Reynolds phenomena caused by the low density at the stratosphere.This regime is essential in HAPS propellers operation. We present a novel optimization algorithm based on coupling the well-known Theodorsen solution with numerical methods based on potential solvers. The Theodorsen distribution gives the $c_l \cdot \sigma_b$ value that each propeller section should have in order to minimize the induced drag. As a consequence of the low Reynolds regime, the aerodynamic coefficients of each section's airfoil varies with the Reynolds number, so there is an additional design variable to take into account. If the chord of a given blade section is changed, it will result in a different lift coefficient and aerodynamic efficiency. With a careful selection of the chord, the highest aerodynamic efficiency can be chosen, so a determined cost function can be minimized.

The present method is focused on the preliminary design, minimizing the computational cost. There is no need to perform CFD simulations or include experimental data, although these tools are beneficial, and they could increase the accuracy of the final design. Due to its low computational time, our method makes possible to perform a parametric sweep, in order to find the optimal diameter and advance ratio. Different combinations of wind speed, thrust re-

Please cite this article in press as: García-Gutiérrez, A., Gonzalo, J., Domínguez, D., López, D., & Escapa, A. (2020). Aerodynamic optimization of propellers for High Altitude Pseudo-Satellites. *Aerospace Science and Technology*, 96, 105562, 10.1016/j.ast.2019.105562

quirements, airfoils and number of blades can be easily checked. Moreover, different cost functions $F(\mathrm{Re})$ can be easily implemented following the same algorithm, like $F(\mathrm{Re}) = c_l/c_d$ or $F(\mathrm{Re}) = c_l^{3/2}/c_d$.

As a case of study, a propeller based on NACA4412 airfoil has been designed for its use in a small airship. The proposed algorithm achieves an increment of more than 5% in the propeller efficiency when compared to a desig created using traditional methods. This can be translated into an increment in the range, endurance or/and payload. Payload increments as high as 25% can be reached.

The structure of the new design method opens the possibility to increase the global performance of the HAPS propeller using more complex cost functions e.g., penalizing too high/low rotational velocity, the total mass, etc. Future studies will be performed implementing these alternative cost functions to integrate the propeller with electric motors [53]. It will also allow multi-point optimization taking into account the different operational conditions that the platform could encounter e.g., different wind speeds and altitudes or including the variability of the aerodynamic coefficients.

The proposed algorithm is a valuable tool for the preliminary design of stratospheric propellers. During the initial phase of the project, many different configurations are considered, there are numerous design changes, and it is important to estimate the best approach for everyone as quickly and accurately as possible. It has been specially designed to improve the efficiency of HAPS propellers and its implementation has shown a significant enhancement in the mission performance.

Acknowledgements

The authors acknowledge the valuable suggestions of the anonymous referees that helped to enhance the manuscript.

Please cite this article in press as: García-Gutiérrez, A., Gonzalo, J., Domínguez, D., López, D., & Escapa, A. (2020). Aerodynamic optimization of propellers for High Altitude Pseudo-Satellites. *Aerospace Science and Technology*, 96, 105562, 10.1016/j.ast.2019.105562

Declaration of Competing Interest

The authors declare that there is no conflict of interests regarding the publication of this article.

References

[1] N. McKeegan, Odysseus: Aurora's radical, unlimited endurance, solar powered aircraft (2008).

[2] F. A. d'Oliveira, F. C. L. d. Melo, T. C. Devezas, High-altitude platforms—present situation and technology trends, Journal of Aerospace Technology and Management 8 (3) (2016) 249–262.

[3] D.-M. Kim, Korea stratospheric airship program and current results, in: AIAA's 3rd Annual Aviation Technology, Integration, and Operations (ATIO) Forum, 2003, p. 6782.

[4] G. Ilieva, J. C. Páscoa, A. Dumas, M. Trancossi, A critical review of propulsion concepts for modern airships, Central European Journal of Engineering 2 (2) (2012) 189–200. doi:10.2478/s13531-011-0070-1.

[5] B. J. Brelje, J. R. R. A. Martins, Electric , Hybrid , and Turboelectric Fixed-Wing Aircraft : A Review of Concepts , Models , and Design Approaches (June).

[6] J. Gonzalo, D. López, D. Domínguez, A. García, A. Escapa, On the capabilities and limitations of high altitude pseudo-satellites, Progress in Aerospace Sciences 98 (2018) 37–56. doi:10.1016/j.paerosci.2018.03.006. URL `https://doi.org/10.1016%2Fj.paerosci.2018.03.006`

[7] D. L. Lisoski, M. B. Tischler, Solar powered stratospheric research aircraft: Flight test and system identification., STAR.

[8] T. E. Noll, J. M. Brown, M. E. Perez-Davis, S. D. Ishmael, G. C. Tiffany, M. Gaier, Investigation of the Helios Prototype Aircraft Mishap, Tech. rep. (2004).

Please cite this article in press as: García-Gutiérrez, A., Gonzalo, J., Domínguez, D., López, D., & Escapa, A. (2020). Aerodynamic optimization of propellers for High Altitude Pseudo-Satellites. *Aerospace Science and Technology*, 96, 105562, 10.1016/j.ast.2019.105562

[9] Airbus Defence, Zephyr: Focus of an aircraft. endurance of a satellite.

[10] A. Boscaleri, F. Castagnoli, P. Rissone, M. Corti, Stratobus: a multiuser platform system for making access to ldb flight easier and cheaper, European Space Agency,(Special Publication) ESA SP 671 (2008) 209–213.

[11] M. Wu, Z. Shi, T. Xiao, H. Ang, Energy optimization and investigation for z-shaped sun-tracking morphing-wing solar-powered uav, Aerospace Science and Technology 91 (2019) 1 – 11. doi:https://doi.org/10.1016/j.ast.2019.05.013.
URL http://www.sciencedirect.com/science/article/pii/S1270963818326294

[12] A. Dumas, F. Pancaldi, F. Anzillotti, M. Trancossi, High altitude platforms for telecommunications: Design methodology, in: SAE Technical Paper, SAE International, 2009. doi:10.4271/2009-01-3159.
URL https://doi.org/10.4271/2009-01-3159

[13] J. D. Mattingly, W. H. Heiser, D. T. Pratt, Aircraft engine design, AIAA Education Series, Reston, Virginia, 2002, Ch. The Design Process.

[14] J. Morgado, M. Abdollahzadeh, M. Silvestre, J. Páscoa, High altitude propeller design and analysis, Aerospace Science and Technology 45 (2015) 398–407. doi:10.1016/j.ast.2015.06.011.
URL https://doi.org/10.1016%2Fj.ast.2015.06.011

[15] C. N. Adkins, R. H. Liebeck, Design of optimum propellers, Journal of Propulsion and Power 10 (5) (1994) 676–682. doi:10.2514/3.23779.
URL http://arc.aiaa.org/doi/10.2514/3.23779

[16] J. Winslow, H. Otsuka, B. Govindarajan, I. Chopra, Basic Understanding of Airfoil Characteristics at Low Reynolds Numbers (104–105), Journal of Aircraft (2017) 1–12doi:10.2514/1.C034415.
URL https://arc.aiaa.org/doi/10.2514/1.C034415

[17] C. Badrya, B. Govindarajan, I. Chopra, Correction: Basic understanding of unsteady airfoil aerodynamics at low reynolds numbers, in: 2018 AIAA

Please cite this article in press as: García-Gutiérrez, A., Gonzalo, J., Domínguez, D., López, D., & Escapa, A. (2020). Aerodynamic optimization of propellers for High Altitude Pseudo-Satellites. *Aerospace Science and Technology*, 96, 105562, 10.1016/j.ast.2019.105562

Aerospace Sciences Meeting, American Institute of Aeronautics and Astronautics, 2018. doi:10.2514/6.2018-2061.c1.
URL https://doi.org/10.2514%2F6.2018-2061.c1

[18] R. Ma, B. Zhong, P. Liu, Optimization design study of low-reynolds-number high-lift airfoils for the high-efficiency propeller of low-dynamic vehicles in stratosphere, Science China Technological Sciences 53 (10) (2010) 2792–2807. doi:10.1007/s11431-010-4087-0.
URL https://doi.org/10.1007%2Fs11431-010-4087-0

[19] J. Liu, S. Luo, Navier-stokes equations based flow simulations of low reynolds number propeller for unmanned aerial vehicle, in: 55th AIAA Aerospace Sciences Meeting, American Institute of Aeronautics and Astronautics, 2017. doi:10.2514/6.2017-0728.
URL https://doi.org/10.2514%2F6.2017-0728

[20] T. Theodorsen, The theory of propellers.

[21] Q. R. Wald, The aerodynamics of propellers, Progress in Aerospace Sciences 42 (2) (2006) 85–128. doi:10.1016/j.paerosci.2006.04.001.
URL https://doi.org/10.1016%2Fj.paerosci.2006.04.001

[22] J. Morgado, M. Â. R. Silvestre, J. C. Páscoa, Validation of new formulations for propeller analysis, Journal of Propulsion and Power 31 (1) (2015) 467–477. doi:10.2514/1.b35240.
URL https://doi.org/10.2514%2F1.b35240

[23] R. MacNeill, D. Verstraete, Blade element momentum theory extended to model low reynolds number propeller performance, The Aeronautical Journal 121 (1240) (2017) 835–857. doi:10.1017/aer.2017.32.
URL https://doi.org/10.1017%2Faer.2017.32

[24] F. Mahmuddin, S. Klara, H. Sitepu, S. Hariyanto, Airfoil lift and drag extrapolation with viterna and montgomerie methods, Energy Procedia

Please cite this article in press as: García-Gutiérrez, A., Gonzalo, J., Domínguez, D., López, D., & Escapa, A. (2020). Aerodynamic optimization of propellers for High Altitude Pseudo-Satellites. *Aerospace Science and Technology*, 96, 105562, 10.1016/j.ast.2019.105562

105 (2017) 811–816. doi:10.1016/j.egypro.2017.03.394.
URL https://doi.org/10.1016%2Fj.egypro.2017.03.394

[25] H. Dumitrescu, V. Cardoş, A. Dumitrache, Modelling of inboard stall delay due to rotation, Journal of Physics: Conference Series 75 (2007) 012022. doi:10.1088/1742-6596/75/1/012022.
URL https://doi.org/10.1088%2F1742-6596%2F75%2F1%2F012022

[26] J. Morgado, R. Vizinho, M. A. Silvestre, J. C. Páscoa, XFOIL vs CFD performance predictions for high lift low Reynolds number airfoils, Aerospace Science and Technology 52 (2016) 207–214. doi:10.1016/j.ast.2016.02.031.

[27] D. Park, Y. Lee, T. Cho, C. Kim, Design and performance evaluation of propeller for solar-powered high-altitude long-endurance unmanned aerial vehicle, International Journal of Aerospace Engineering 2018 (2018) 1–23. doi:10.1155/2018/5782017.
URL https://doi.org/10.1155%2F2018%2F5782017

[28] J. Jiao, B.-F. Song, Y.-G. Zhang, Y.-B. Li, Optimal design and experiment of propellers for high altitude airship, Proceedings of the Institution of Mechanical Engineers, Part G: Journal of Aerospace Engineering 232 (10) (2017) 1887–1902. doi:10.1177/0954410017704217.
URL https://doi.org/10.1177%2F0954410017704217

[29] S. Goldstein, On the Vortex Theory of Screw Propellers, Proceedings of the Royal Society A: Mathematical, Physical and Engineering Sciences 123 (792) (1929) 440–465. doi:10.1098/rspa.1929.0078.
URL http://rspa.royalsocietypublishing.org/cgi/doi/10.1098/rspa.1929.0078

[30] H. S. Ribner, S. P. Foster, Ideal Efficiency of Propellers: Theodorsen Revisited, Journal of Aircraft 27 (9) (1990) 810–819. doi:10.2514/3.45941.

[31] N. Batista, R. Melicio, V. Mendes, Darrieus-type vertical axis rotary-wings with a new design approach grounded in double-multiple streamtube performance prediction model, AIMS Energy 6. doi:10.3934/energy.2018.5.673.

Please cite this article in press as: García-Gutiérrez, A., Gonzalo, J., Domínguez, D., López, D., & Escapa, A. (2020). Aerodynamic optimization of propellers for High Altitude Pseudo-Satellites. *Aerospace Science and Technology*, 96, 105562, 10.1016/j.ast.2019.105562

[32] N. Batista, R. Melicio, V. Mendes, Darrieus vertical axis wind turbines: methodology to study the self-start capabilities considering symmetric and asymmetric airfoils, Research on Engineering Structures and Materials 4 (2018) 189–217. doi:10.17515/resm2017.39ds0108.

[33] L. D. Koch, Design and Performance Calculations of a Propeller for Very High Altitude Flight, no. February, 1998.

[34] J. S. Monk, A Propeller Design and Analysis Capability Evaluation for High Altitude Application, Master, University of the Witwatersrand (2010).

[35] P. B. S. Lissaman, Low-reynolds-number airfoils (1983) 223–239.

[36] M. Drela, XFOIL: An Analysis and Design System for Low Reynolds Number Airfoils (2011) 1–12.

[37] M. Hepperle, Javafoil-analysis of airfoils, See http://www. mh-aerotools. de/airfoils/javafoil. htm.

[38] R. Eppler, D. M. Somers, A computer program for the design and analysis of low-speed airfoils.

[39] J. C. Chua, N. S. Lopez, G. Augusto, Numerical and statistical analyses of aerodynamic characteristics of low Reynolds number airfoils using Xfoil and JMP, AIP Conference Proceedings 1905. doi:10.1063/1.5012235.

[40] O. Günel, E. Koç, T. Yavuz, CFD vs. XFOIL of airfoil analysis at low reynolds numbers, 2016 IEEE International Conference on Renewable Energy Research and Applications, ICRERA 2016 5 (2016) 628–632. doi:10.1109/ICRERA.2016.7884411.

[41] X. Zheng, X. Wang, Z. Cheng, D. Han, The efficiency analysis of high-altitude propeller based on vortex lattice lifting line theory, The Aeronautical Journal 121 (1236) (2016) 141–162. doi:10.1017/aer.2016.112.
URL https://doi.org/10.1017%2Faer.2016.112

Please cite this article in press as: García-Gutiérrez, A., Gonzalo, J., Domínguez, D., López, D., & Escapa, A. (2020). Aerodynamic optimization of propellers for High Altitude Pseudo-Satellites. *Aerospace Science and Technology*, 96, 105562, 10.1016/j.ast.2019.105562

[42] J. Brandt, M. Selig, Propeller performance data at low reynolds numbers, in: 49th AIAA Aerospace Sciences Meeting including the New Horizons Forum and Aerospace Exposition, American Institute of Aeronautics and Astronautics, 2011. doi:10.2514/6.2011-1255.
URL https://doi.org/10.2514%2F6.2011-1255

[43] M. Silvestre, J. Morgado, P. Alves, P. Santos, P. Gamboa, J. Páscoa, Propeller Performance Measurements at Low Reynolds Numbers, International Journal of Mechanics 9 (April) (2015) 154–166.
URL http://www.naun.org/main/NAUN/mechanics/2015/a372003-136.pdf

[44] T. Liu, A. Oyama, K. Fujii, Scaling analysis of propeller-driven aircraft for mars exploration, Journal of Aircraft 50 (5) (2013) 1593–1604. doi:10.2514/1.c032086.
URL https://doi.org/10.2514%2F1.c032086

[45] T. J. Mueller, L. J. Pohlen, P. E. Conigliaro, B. J. Jansen, The influence of free-stream disturbances on low Reynolds number airfoil experiments, Experiments in Fluids 1 (1) (1983) 3–14. doi:10.1007/BF00282261.

[46] J. F. Marchman, T. D. Werme, Clark-Y Airfoil Performance at Low Reynolds, AI AA-84-0052 Numbers AlAA 22nd Aerospace Sciences Meeting.

[47] M. Simons, Model Aircraft Aerodynamics (1994).

[48] E. J.N, A. Sherman, Airfoil Section Characteristics as Affected by Variations of the Reynold's Number, NACA Report 586.

[49] K. Koca, M. S. Genç, H. H. Açıkel, M. Çağdaş, T. M. Bodur, Identification of flow phenomena over NACA 4412 wind turbine airfoil at low Reynolds numbers and role of laminar separation bubble on flow evolution, Energy 144 (2018) 750–764. doi:10.1016/j.energy.2017.12.045.

[50] W. H. W. Ebisuzaki, J. Janowiak, K. C. Mo, C. Rope-lewski, J. Wang, A. Leetmaa, R. Reynolds, R. Jenne, The NCEP/ NCAR reanalysis

project, Bull. Amer. Meteor. Soc. 77 (1996) 437–471. doi:10.1175/1520-0477(1996)077¡0437:TNYRP¿2.0.CO;2.

[51] A. N. Celik, Energy output estimation for small-scale wind power generators using weibull-representative wind data, Journal of wind engineering and industrial aerodynamics 91 (5) (2003) 693–707.

[52] J. Goss, P. H. Mellor, R. Wrobel, D. a. Staton, M. Popescu, The design of AC permanent magnet motors for electric vehicles: A computationally efficient model of the operational envelope, Power Electronics, Machines and Drives (PEMD 2012), 6th IET International Conference on (2012) 1–6doi:10.1049/cp.2012.0251.

[53] R. MacNeill, D. Verstraete, A. Gong, Optimisation of Propellers for UAV Powertrains, 53rd AIAA/SAE/ASEE Joint Propulsion Conference (July) (2017) 1–25. doi:10.2514/6.2017-5090.
URL https://arc.aiaa.org/doi/10.2514/6.2017-5090

[54] J. Ketcham, S. Multiconference, B. Epps, J. Ketcham, C. Chryssostomidis, Propeller blade stress estimates using lifting line theory.

[55] A. Garrad, Dynamics of wind turbines, Vol. 130, 2010. doi:10.1049/ip-a-1.1983.0080.

[56] E. Buckingham, Dimensional analysis of model propeller tests, Journal of the American Society for Naval Engineers 48 (2) (1936) 147–198. doi:j.1559-3584.1936.tb01423.x.

[57] L. W. Traub, Range and endurance estimates for battery-powered aircraft, Journal of Aircraft 48 (2) (2011) 703–707. doi:10.2514/1.C031027.

Please cite this article in press as: García-Gutiérrez, A., Gonzalo, J., Domínguez, D., López, D., & Escapa, A. (2020). Aerodynamic optimization of propellers for High Altitude Pseudo-Satellites. *Aerospace Science and Technology*, 96, 105562, 10.1016/j.ast.2019.105562